

Cortico-Muscular Phase Connectivity During an Isometric Knee Extension Task in People With Early Parkinson's Disease

Nina Omejc[®], Tomislav Stankovski[®], Manca Peskar, Miloš Kalc[®], Paolo Manganotti, Klaus Gramann[®], Sašo Džeroski[®], and Uros Marusic

Received 1 October 2024; revised 9 December 2024; accepted 5 January 2025. Date of publication 9 January 2025; date of current version 27 January 2025. The work of Nina Omejc and Sašo Džeroski was supported in part by the Slovenian Research Agency via the Research Program Knowledge Technologies under Grant P2-0103; in part by research projects under Grant J1-3033, Grant J2-2505, Grant J2-4452, Grant J2-4660, Grant J3-3070, Grant J4-3095, Grant J5-4575, Grant J7-4636, Grant J7-4637, and Grant N2-0236; in part by the EC via the projects ASSAS under Grant 101059682; in part by ELIAS under Grant 101120237; in part by INQUIRE under Grant 101057499; in part by PARC under Grant 101057014; and in part by TAILOR under Grant 952215. The work of Uros Marusic was supported in part by Horizon Europe under Grant 101120150, in part by the Slovenian Research and Innovation Agency (ARIS): Research Program Kinesiology for Quality of Life under Grant P5-0381, and in part by the Research Project Adaptation and Sensorimotor Processing during Increased Gravity Gradients under Grant J7-4601. (Corresponding author: Nina Omejc.)

This work involved human subjects or animals in its research. Approval of all ethical and experimental procedures and protocols was granted by the IRB of Trieste University Hospital - ASUGI, Trieste, Italy, under ASUGI Protocol No. 106/2021, approved on 20.12.2022, and on ClinicalTrials.Gov under Code No. NCT05477654, and performed in line with the Declaration of Helsinki.

Nina Omejc is with the Department of Knowledge Technologies, Jožef Stefan Institute, 1000 Ljubljana, Slovenia, and also with the Jožef Stefan International Postgraduate School, 1000 Ljubljana, Slovenia (e-mail: nina.omejc@ijs.si).

Tomislav Stankovski is with the Faculty of Medicine, Ss. Cyril and Methodius University in Skopje, 1000 Skopje, Macedonia, and also with the Department of Physics, Lancaster University, LA1 4YB Lancaster, U.K.

Manca Peskar is with the Institute for Kinesiology Research, Science and Research Centre Koper, 6000 Koper, Slovenia, and also with the Department of Psychology and Ergonomics, Faculty V–Mechanical Engineering and Transport Systems, Technische Universität Berlin, 10623 Berlin, Germany.

Miloš Kalc is with the Institute for Kinesiology Research, Science and Research Centre Koper, 6000 Koper, Slovenia.

Paolo Manganotti is with the Clinical Unit of Neurology, Department of Medical, Surgical and Health Sciences, Cattinara Hospital, University of Trieste, 34149 Trieste, Italy.

Klaus Gramann is with the Department of Psychology and Ergonomics, Faculty V–Mechanical Engineering and Transport Systems, Technische Universitat Berlin, 10623 Berlin, Germany.

Sašo Džeroski is with the Department of Knowledge Technologies, Institut Jozef Stefan, 1000 Ljubljana, Slovenia.

Uros Marusic is with the Institute for Kinesiology Research, Science and Research Centre Koper, 6000 Koper, Slovenia, and also with the Department of Health Sciences, Alma Mater Europaea University, 2000 Maribor, Slovenia.

This article has supplementary downloadable material available at https://doi.org/10.1109/TNSRE.2025.3527578, provided by the authors. Digital Object Identifier 10.1109/TNSRE.2025.3527578

Abstract - Introduction: Cortico-muscular (CM) interactions provide insights into the flow of information between neural and motor systems. Reduced CM phase connectivity has been linked to functional impairments in clinical populations. Objective: This study aimed to determine whether similar reductions occur in individuals with Parkinson's disease (PD), characterized primarily by motor impairments. Specifically, it aimed to characterize electroencephalography (EEG) and electromyography (EMG) power spectra during a motor task, assess CM phase connectivity, and explore how an additional cognitive task modulates these measures. Methodology: Fifteen individuals with early-stage PD and sixteen age-matched controls performed an isometric knee extension task, a cognitive task, and a combined dual task, while EEG (128 channels) and EMG (2x32 channels) were recorded. CM phase connectivity was analyzed through phase coherence and phase dynamics modeling. Results: The strongest CM phase coherence was observed in the lower beta band (12.5-15 Hz) over the Cz electrode and was significantly higher in healthy controls compared to individuals with PD during the motor task. The phase dynamics model additionally revealed stronger directional coupling from the Cz electrode to the active muscle, than in the reverse direction, with less pronounced phase coupling in the PD cohort. Notably, CM phase coherence exhibited distinct scalp topography and spectra characteristics compared to the EEG power spectrum, suggesting different mechanisms underlying Parkinsonian pathological beta power increase and CM phase connectivity. Lastly, despite high inter-individual variability, these metrics may prove useful for personalized assessments, particularly in people with heightened CM connectivity.

Index Terms—Cortico-muscular connectivity, dynamic Bayesian inference, early-stage Parkinson's disease, EEG, EMG, isometric knee extension, motor-cognitive dual tasks, phase coherence, phase dynamics model.

I. INTRODUCTION

PARKINSON'S disease (PD) is a neurodegenerative disorder, characterized by a variety of non-motor symptoms, such as cognitive decline, depression, and disturbance of sleep [1], [2], but mainly by motor symptoms such as bradykinesia, rigidity, and tremor [3], [4]. These motor symptoms have been associated with enhanced beta-band (13–30 Hz) oscillations in

the basal ganglia, cortico-basal ganglia loop and cerebral cortex [9], [10], [11], [12], [13], [14], [15], [16]. This connection is particularly evident in studies showing that both pharmacological interventions [17] and deep brain stimulation [18], [19] effectively reduce the beta-band over-synchronization in afferents to the motor cortex, and alleviate motor symptoms. Given the observed alterations in brain rhythms and motor functioning, combined electroencephalography (EEG) and electromyography (EMG) present a promising approach for investigating functional alterations in PD and exploring their potential as diagnostic tools.

Optimal screening tools for early diagnosis of PD are still lacking. The presymptomatic phase of Parkinson's disease pathology in olfactory structures and enteric nervous system starts more than a decade before the onset of typical clinical manifestations and diagnosis [5], [6]. Currently, patients are predominantly diagnosed using the Movement Disorder Society Unified Parkinson's Disease Rating Scale (MDS-UPDRS) [99], which primarily focuses on assessing motor deficits. Even at the stages, where the motor symptoms are already present, detection remains challenging, with movement-disorder specialists encountering error rates of approximately 20 % [6], [8]. For this reason, researchers have been working to identify new, specific, and sensitive biomarkers through direct measures such as magnetic resonance imaging (MRI), positron emission tomography (PET), cerebrospinal fluid (CSF) analysis, and genetic studies [6].

The analysis of brain activity using combined EEG and EMG has not yet been adopted in the diagnostic or examination protocols for PD [6]. Both methods are cost-effective, portable, and capable of recording activity during movement. While EEG is limited in its capacity to measure the activity of subcortical nuclei, some of which the PD directly impacts, cortical regions are also indirectly influenced by activity in these nuclei. The prefrontal association areas, crucial for cognitive functions, are influenced by brainstem nuclei via connections to the limbic loop centers. Additionally, the degradation of the substantia nigra affects premotor and motor areas by disrupting the nigro-striatal pathway, which in turn affects the cortico-striatal pathway projecting to the motor cortex [3], [7], [20], [21].

A combined EEG and EMG measurement assesses both central and peripheral neural activities, facilitating the investigation of their functional interactions during movement. It can quantify the synchronization between sensorimotor cortical areas and motor neuron pools, reflecting the cortico-spinal interaction and central drive to skeletal muscles. In this study, we aim to explore the CM connectivity in people with early-stage PD, to determine whether detectable changes in CM connectivity are present.

Various metrics and models have been developed to capture the type, strength, and direction of cortico-cortical connectivity, such as phase-amplitude coupling [19], magnitude-squared coherence [22], [23], phase coherence or phase locking value [60], [61], [62], and autoregressive modeling techniques such as Granger causality, directed transfer function [63], [64] and (nonlinear) partial directed coherence [65], [66], [67].

Other methods include model-free methods that are based on information theory, such as mutual information, transfer entropy [68], [69], [70] or (time-frequency) maximal information coefficient [71], [72]. Moreover, various methods for assessing effective connectivity have been explored, where the parameters of preselected models are estimated based on empirical data. Notable examples of these methods are dynamic causal modeling [73] and dynamical Bayesian inference [74], [75], [76].

One of the well-established connectivity measures for CM connectivity is magnitude-squared coherence [22], [23], [24], [25]. Strong CM magnitude-squared coherence has been observed in the beta frequency range (13-30 Hz) between different areas of sensorimotor cortex and active peripheral muscles, predominantly during sustained voluntary contractions [23], [26], [27], [28], [29], [30], [31], [32], [33], [34]. Numerous studies have investigated CM connectivity using magnitude-squared coherence, but the method has limitations. These include its symmetry, which prevents assessing the direction of connectivity between signals, and its linearity, which fails to capture the complexity of the nonlinear sensorimotor system [59]. Moreover, magnitude-squared coherence analysis can detect whether two processes exhibit oscillations within the same frequency range, but cannot separate the effects of amplitude and phase [61] or determine whether these oscillations are independent or coupled [62], [78]. In this study, we chose to evaluate functional connectivity within the phase domain, as it enables direct exploration of temporal relationships between neural signals [77] and leverages the time-domain strengths of EEG and EMG methodologies. Phase coherence or phase locking value can measure the consistency of the phase difference between two signals over time and across frequencies, giving additional insights into the phase coupling or synchrony between signals. This has been proposed as essential for processes such as perceptual binding, long-range synchronization, or control of the excitability in distant neuron groups [61], [79], [80], [81], [82]. Phase analysis has already been used in examining CM interactions [83], [84], [85], also using more general multi-spectral phase coherence [86], [87], but we could not find any research on PD.

Additionally, we employ phase dynamics modeling to overcome the symmetry limitation of phase coherence and its inability to assess coupling directionality. We aim to model the CM phase connectivity as a system of coupled phase oscillators following the Kuramoto model [88], [89], of which parameters are inferred via dynamical Bayesian inference [74], [75], [76]. This method falls under effective connectivity approaches, where a specified model directly explains the causal dynamics [90]. It allows for a detailed definition of the coupling functions between the signals and enables the determination of the coupling direction between EEG and EMG. The phase dynamics model describes a phase oscillator and its rate of phase change, which is governed by the intrinsic frequency. When coupled to other oscillators, the oscillator is also influenced by their phases via coupling functions. By finding the most influential coupling functions, we can characterize the strength and nature of the signal coupling [91], [92]. The

TABLE I
DEMOGRAPHIC AND CLINICAL CHARACTERISTICS OF PARTICIPANTS

	People with PD		Controls	
	Mean	SD	Mean	SD
Age (years)	63.8	6.2	63.7	7.2
BMI	25.3	4.1	24.6	7.3
Years of Edu.	11.9	3.6	15.5	3.7
MoCA	27.1	1.6	27.3	1.7
UPDRS III	14.7	6.8	-	-
UPDRS Total	27.5	15.9	-	-

BMI: body-mass index, Edu.: Education, MoCA: Montreal Cognitive Assessment Score, UPDRS: Unified Parkinson's Disease Rating Scale.

simplicity and scalability of the phase dynamics model make it well-suited for capturing the oscillatory activity commonly observed in EEG and EMG signals. The method has been previously applied to modeling cortico-cortical connectivity [93], [94], [95], but its application to CM connectivity has not yet been explored.

This study investigates CM phase connectivity in individuals with early-stage PD and age-matched healthy controls during an isometric knee extension task. Alongside the motor task, participants also perform a dual-task condition involving a cognitive, non-verbal -3 subtraction task, which has been demonstrated to influence motor functioning [96], [97], [98]. Our objectives are to: characterize the EEG and EMG power spectra, as well as CM phase connectivity, with a particular focus on the beta-band; assess how the addition of a cognitive task modulates these measures; and evaluate their potential as biomarkers for diagnosis or rehabilitation.

II. METHODOLOGY

A. Participants

A total of 22 people with an early diagnosis of PD (Hoehn and Yahr stage I–II) have been recruited in the study, together with 27 age and gender-matched healthy participants. All patients with PD received anti-parkinsonian medications. Motor performance in all participants was assessed by the MDS-UPDRS scale [99], administered by an experienced neurologist. In the final analysis of this study, data from 15 patients with PD (6 females) and 16 healthy participants (7 females) were included.

Several participants were excluded due to the unavailability of data (some participants did not complete this part of the study), or excessive noise in the collected data. The average and standard deviation of the body-mass index, years of education, the Montreal Cognitive Assessment (MoCA) score, and UPDRS scores are shown in Table I for both cohorts. UPDRS scores are not available for the control cohort.

All participants provided written informed consent prior to the study. The study adhered to the Declaration of Helsinki and received approval from the ethics committee. The study was registered at IRB of Trieste University Hospital - ASUGI, Trieste, Italy (ASUGI protocol number: 106/2021; approved on 20.12.2022) and on ClinicalTrials.Gov under the code NCT05477654.

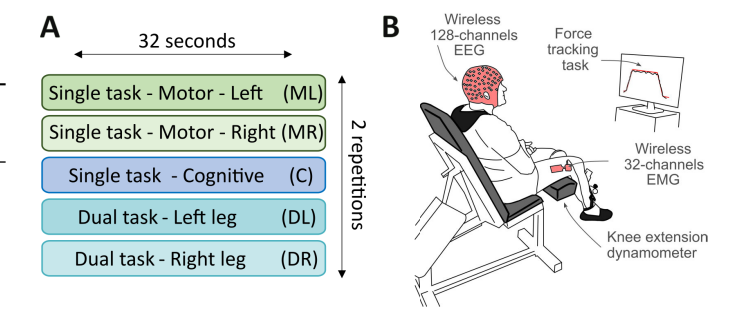


Fig. 1. Overview of experimental tasks. Subfigure A: Schematic representation of the experimental tasks. Subfigure B depicts the motor task, specifically an isometric knee extension task. It was taken and edited with permission from the published study protocol of Marusic et al. [100].

B. Experiment

The experiment was conducted as part of our clinical trial. For a comprehensive description of the methodology and protocols, please refer to Marusic *et al.* [100]. In this part of the experiment, participants engaged in three tasks (see Fig. 1A): a single task - motor, a single task - cognitive, and a dual task, where they had to perform motor and cognitive tasks simultaneously. The motor task was performed with each leg separately.

The motor task is shown in Fig. 1B. Participants had to perform an isometric knee extension task, which involved a 32-second force tracking session with a trapezoidal pattern (6-second rising phase, 20-second sustained phase, 6-second decline phase). The task was performed with the right and left lower limbs separately. Participants were instructed to actively contract their knee extensors to produce force up to 30 % of their maximum voluntary contraction (MVC). A knee extension dynamometer equipped with a force sensor was used to provide feedback to participants. Feedback was shown on the computer screen in front of them, together with the desired force level.

In the cognitive task, participants performed a 32-second non-verbal serial -3 subtraction, starting from a randomly selected number between 300 and 500, reporting only the final result.

The order of limb usage and task conditions was counterbalanced across participants, with the single task conditions performed before the dual task for each limb. Each of the five conditions was repeated twice.

C. EEG and EMG measurements

EEG activity was recorded with a mobile 128-electrode wireless system (CGX, Cognionics Inc., San Diego, USA), following the 10-5 electrode placement system [101]. We used Ag/AgCl wet electrodes, with a 500 Hz sampling rate, 24 bits of resolution, and no filter settings. The electrode impedance was kept below 20 $k\Omega$ for each channel and balanced across all channels within a 5 $k\Omega$ range. Reference and ground electrodes were placed on the right and left mastoids, respectively.

EMG activity was monitored using two wireless 32-channel probes (MUOVI, OT Bioelettronica S.r.l., Torino, Italy), with electrodes positioned on the bilateral *vastus lateralis* muscles. We used Ag/AgCl wet electrodes, with a 2000 Hz sampling

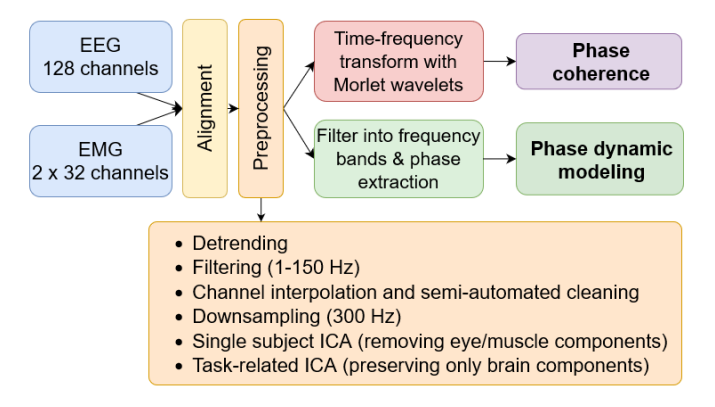


Fig. 2. Analysis diagram, showing the processing workflow of the acquired EEG and EMG signals, including the preprocessing and main connectivity analysis steps.

rate, and no filter settings. The electrode, serving as both the reference and ground, was placed on the patella of each knee. EEG and EMG signal synchronization was achieved by a common TTL pulse that was sent via the PowerLab data acquisition toolbox in LabChart software (AD Instruments, Sydney, Australia) to both the EMG and EEG systems. This allowed us to achieve offline alignment of the signals with sub-millisecond accuracy.

A schematic overview of the EEG and EMG data analysis pipeline is shown in Fig. 2. The code used to preprocess the data and calculate connectivity measures is available on GitHub at https://github.com/NinaOmejc/cmcpd.git. It was written in Matlab (version 2023a, The Math Works, USA), using EEGLAB toolbox [102] for preprocessing, Multiscale Oscillatory Dynamics Analysis software [103] for phase connectivity analysis and custom scripts. To synchronize the data, EMG data was resampled from 2000 Hz to 500 Hz and aligned with the EEG using a common TTL pulse. Following the alignment, extensive preprocessing was applied to both the EEG and EMG data.

1) Preprocessing: We first excluded non-task data and removed flat-line EMG electrodes. Next, we removed the trend in the signal by subtracting the moving average calculated over 10-second time windows. The data were then filtered using a high-pass filter with a 1 Hz cut-off frequency and a low-pass filter with a 150 Hz cut-off frequency (Hamming windowed sinc FIR filters) [102]. We employed the Zaplineplus method to remove line noise [104], [105]. EEG electrodes with excessive artifacts were automatically detected using the Clean Rawdata EEGLAB plug-in with subsequent manual inspection. The final set of bad electrodes was interpolated using spherical spline interpolation. On average, we interpolated 24/128 electrodes per data set (SD=10.8). After channel interpolation, another manual inspection was conducted to remove any bad data segments. Subsequently, the EEG data was re-referenced to the average reference, and both EEG and EMG data were downsampled to 300 Hz. Table in Appendix I (Supplementary Material) presents the final amount of clean data, categorized by cohort and task.

As the final two preprocessing steps, two independent component analyses (ICA) were performed on EEG data, using *runica* (*Infomax*) algorithm in EEGLAB toolbox. In the first ICA, data from each participant (over all tasks) were concatenated to facilitate the removal of ocular, muscular, and cardiac independent components (ICs) specific to each individual. ICs were selected with the help of ICLabel plug-in [106], which provides a classification label and its probability. Additionally, we also considered scalp topography, the scalp data variance accounted for, dipole position, power spectrum, and time series itself. On average, 32 ICs were removed (SD = 9) per participant. Remained ICs were projected back to the scalp electrodes.

In the second ICA step, we merged all EEG data from a single task across all participants to identify task-specific brain components. With the same approach as for the first ICA step, we manually retained the top 20 ICs across all datasets. Again, kept ICs were projected back to the electrodes.

Importantly to note, we did not rectify EMG data to not additionally modify the frequency spectrum and the phase of the signals [108], [109], [110]. However, for further analysis, we reduced the data dimensionality by averaging all 32 EMG time series for each leg. Beforehand, we confirmed that prior averaging had a minimal impact on the results [see Appendix II (Supplementary Material)].

2) Continuous wavelet transform: To calculate phase coherence, we first transformed the continuous, cleaned EEG and EMG data into the time-frequency domain. We calculated continuous wavelet transform, $W_x(\omega, t)$, of a signal x(t) at angular frequency ω and time t as in [94], [103]:

$$W_{x}(\omega, t) = \int_{0}^{\infty} \psi(\omega(u - t)) x(u) \omega \, du, \tag{1}$$

$$\psi(u) = \frac{1}{2\pi} \left(e^{i2\pi f_0 u} - e^{\frac{(2\pi f_0)^2}{2}} \right) e^{-\frac{u^2}{2}}.$$
 (2)

We employed a Morlet wavelet $\psi(u)$ with a central frequency parameter $f_0=1$, 30 voices per octave, and a zero-mean property ($\int \psi(t) dt = 0$). Symbol i is the imaginary unit. The frequency boundaries were 4–90 Hz. EEG wavelet power $|\mathcal{W}_x(\omega,t)|^2$ was computed for each scalp electrode, and EMG wavelet power from the averaged time series of 32 electrodes per leg.

Due to the limited number of trial repetitions, we averaged the wavelet power over time. To further conduct group analysis, we performed a z-transformation on the EEG wavelet power, across all electrodes and frequencies. This standardization ensured fair averaging across subjects by focusing on relative, not absolute, power values across electrodes and frequencies. Further details on z-transformation are described in Appendix III (Supplementary Material).

After standardization, we simplified the results by averaging the data from the left and right muscle contractions. This reduction transformed the initial five conditions (see Fig. 1A) into three consolidated task categories: a motor task, a cognitive task, and a dual task. Before combining the data, we checked for lateral differences above the central brain region but found none, likely due to the chosen motor task. The neuronal population responsible for knee extension movement is located medially within the motor cortex gyri [111], with

regions from both hemispheres positioned so closely that EEG could not distinguish positional differences.

Finally, to conduct statistical comparisons on our 2-by-3 design with non-normally distributed values, we computed p-values using the Scheirer–Ray–Hare (SRH) test [112] at each frequency. To account for multiple comparisons, we applied the false discovery rate (FDR) correction [113]. Differences were considered significant if p-values were below the significance level $\alpha=0.05$. We examined differences in the main factors of task and cohort, as well as their interaction effect. We further assessed the pairwise significance using the non-parametric Wilcoxon test [115].

3) Phase coherence calculation: Phase coherence or phase locking value [60], [114] is a statistical method that computes how consistent or stable the phase difference between the two signals is over time, regardless of whether the actual phase difference is zero [61], [62]. Phase coherence $\mathcal{PC}(\omega)$ was calculated pairwise between each EEG electrode and the averaged EMG of each leg, following Eq. (3).

$$\mathcal{PC}(\omega) = \left| \frac{1}{T} \sum_{t=1}^{T} e^{i(\theta_{eeg}(\omega, t) - \theta_{emg}(\omega, t))} \right|, \tag{3}$$

where $\theta_x(\omega, t)$ is the angle of $\mathcal{W}_x(\omega, t)$, T represents the number of time points and ω the angular frequency. Phase coherence was calculated at each time point t but was then averaged over both trials.

We conducted z-transformation and statistical analyses over frequencies using the same approach as in the wavelet power analysis. Additionally, we extracted individual maximum low-beta (13–20 Hz) values and statistically compared the distributions between cohorts and tasks, using a pairwise non-parametric Wilcoxon rank-sum test [115].

To assess the statistical significance of observed patterns against random phase coherence, we performed surrogate analysis [116]. To create the surrogate time series, we used the cycle phase permutation surrogates [116], which are designed for phase dynamics. We created N=30 surrogate time series per participant, which resulted in N*(N-1)/2=435 phase coherence surrogates.

4) Phase dynamics modeling: We further modeled phase connectivity between two signals as coupled phase oscillators. The model was based on the Kuramoto model [88], [89], which is well-suited for biological signals due to their inherent rhythmicity [91]. The phase dynamics of two coupled oscillators *i* and *j* are described in Eq. (4):

$$\dot{\theta}_i = \omega_i + q_i(\theta_i, \theta_j) + \xi_i,
\dot{\theta}_j = \omega_j + q_j(\theta_i, \theta_j) + \xi_j.$$
(4)

A pair of differential equations tell how the phase θ_i of the signal i changes with its intrinsic frequency ω_i and by the influences from other oscillators, as described by $q_i(\theta_i,\theta_j)$. The term ξ corresponds to the white noise. A similar relationship applies reciprocally to oscillator j. An extended version of the phase dynamics model with 24 coupling terms inside the coupling function $q_i(\theta_i,\theta_j)$, that was fitted to the data, is shown in Appendix IV (Supplementary Material).

We first applied a 4th-order Butterworth filter with a zerophase distortion to the data, selecting the low beta-band range (12.5–20 Hz). We then extracted the instantaneous protophase signals using the Hilbert transform and converted them to phase signals via the protophase-to-phase transformation [117]. We then fitted the extended phase dynamics model to the phase signals of each EEG electrode on the scalp and the average EMG signal of each leg.

We applied dynamical Bayesian inference to reconstruct the matrix of coupling coefficients and noise strength, fully characterizing the oscillator coupling [75], [76], [94]. Further details of the inference method can be found in Appendix V (Supplementary Material).

The model was inferred over the 3-second time windows, with a 50 % overlap. The main outcome of dynamical Bayesian inference analysis is a $N \times K$ matrix, where K = 50 represents the inferred coefficients c_k , which include the oscillator's intrinsic frequency and the coupling terms. Each of the two equations contributes 25 coefficients, which are calculated for all N time windows. Due to the initial convergence of the prior, we removed the results of the first 5 windows from the final analysis.

After the parameter inference, we aimed to identify the most significant coupling terms in the model. To do this, we calculated the average absolute values of each of the 24 coefficients across all participants and compared them to distributions of surrogate absolute parameter values. The surrogates were calculated as explained in the previous subsection for phase coherence calculation. Coupling terms with absolute values above the surrogate threshold (average + 2 SD) over all categories were considered dominant coupling terms.

To quantify the coupling strength between two oscillators i and j, we calculated the Euclidean norm of the dominant coupling terms: $\sigma^{(i,j)} = \sqrt{\sum_{m \in M} (c_m^{(i,j)})^2}$, where M denotes the set of indices corresponding to the dominant coupling terms

Lastly, we compared the individual shapes and variances of the coupling functions. To accomplish this, we calculated the similarity index [118], which represents the correlation coefficient between the coupling functions: $\rho = \frac{\langle \vec{q}_1 \, \vec{q}_2 \rangle}{||q_1|| \, ||q_2||}$, where $\langle \cdot \rangle$ denotes spatial averaging over the 2D domain, \tilde{q} denotes $q - \langle q \rangle$, and $||q|| = \sqrt{\langle qq \rangle}$, with additional conditions $0 <= \phi_1$ and $\phi_2 <= 2\pi$. We calculated the similarity indices between the median coupling functions of each cohort and the dominant coupling function, as well as among the median coupling functions of each cohort.

III. RESULTS

We conducted an experiment involving an isometric knee extension task, with and without an additional cognitive component. It included 16 people with Parkinson's disease (PD) and 15 matched healthy controls (HC). Following data collection and preprocessing, we computed power frequency spectra and cortico-muscular (CM) phase coherence and modeled the CM data as coupled phase oscillators by inferring the phase dynamics model using dynamical Bayesian inference. The results are presented in the same sequence.

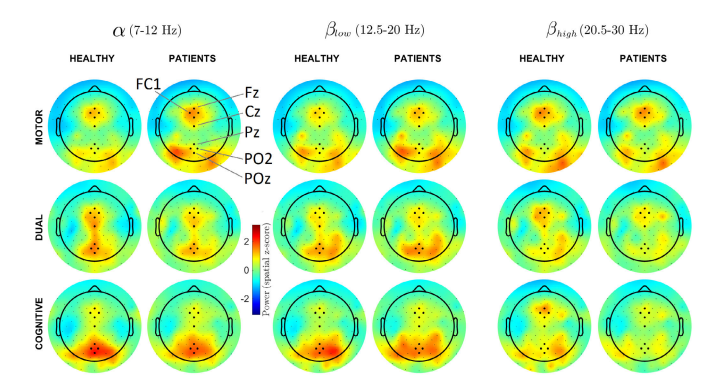


Fig. 3. Topological distribution of relative EEG wavelet power. EEG power distribution is shown across tasks (motor, dual, cognitive), frequency bands (alpha, beta low, and beta high), and cohorts (people with PD and healthy controls) over the scalp electrodes. The power values were standardized across electrodes and frequencies and averaged across the trial length, trials, and participants within the cohort. The black dots on the plots correspond to electrode positions. Some dots over the strongest activity regions are enlarged for easier comparison. The five groups of enlarged electrodes are the fronto-central cluster (FCz, Fz, FC1, FC2), central electrode Cz, and parieto-occipital cluster (Pz, POz, PO1, PO2). Note that the values are z-scored, making them relative to each other, and, consequently, include negative values.

A. Wavelet power frequency spectra

First, we show the results of EEG wavelet time-frequency transformation. Fig. 3 shows the topographical distribution of standardized EEG power for three frequency bands: alpha (7–12 Hz), beta low (12.5–20 Hz), beta high (20.5–30 Hz), whereas the topographical distributions of power in gamma low (30.5–48 Hz) and gamma high (52–90 Hz) can be seen in Appendix VI (Supplementary Material).

An initial observation is that each task exhibits a distinct topographical power distribution that is consistent across both cohorts and, to some extent, across frequency bands. During the motor task (first row in Fig. 3), the highest relative power was observed over the fronto-central region, (at enlarged electrodes Fz, FCz, FC1, and FC2). High rhythmic activity in this region spanned a range of frequencies, from alpha to low gamma. In the dual task, the fronto-central region continued to show high relative power (second row in Fig. 3) but it was generally lower compared to the single motor task. During the cognitive task (third row in Fig. 3), activity over sensorimotor areas decreased even further, and only relatively strong high beta power was observed in a healthy cohort.

Conversely, the medial parieto-occipital region (enlarged electrodes Pz, POz, PO1, and PO2) exhibited the highest activation during the cognitive task, particularly in the alpha and low beta bands. This strong rhythmic activity was less pronounced during the dual task and even less so during the single motor task.

To further quantify the differences, we looked at frequency spectra at the three regions with the highest activity: frontocentral cluster, central Cz electrode, and parieto-occipital cluster, and plotted them in Fig. 4. The frequency spectra match the topographical plots, illustrating distinct patterns of activity across different brain regions, independently of the cohort. In the fronto-central region, the strongest power was observed during the motor task; in the central region, peak

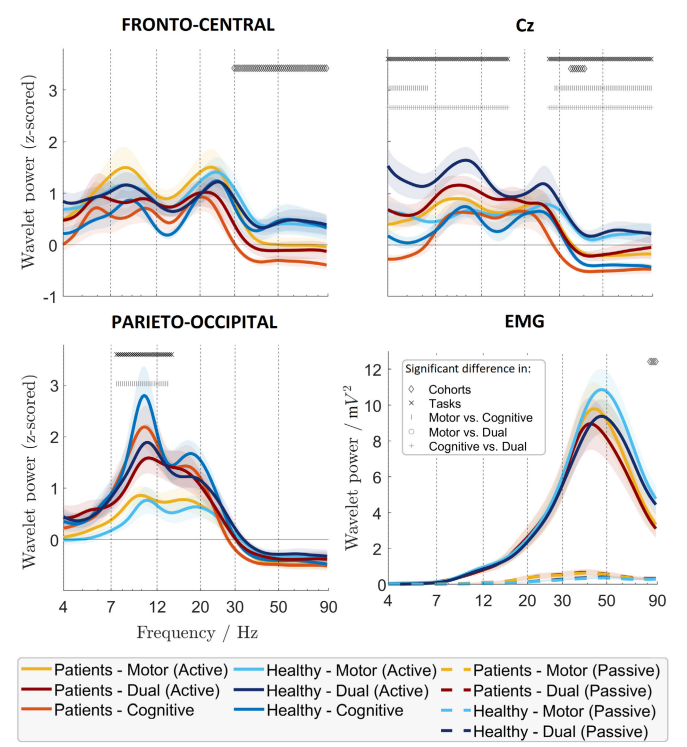


Fig. 4. Wavelet power spectra of EEG & EMG signals, categorized by region, cohort, and task. The subplots present spatially standardized EEG power spectra for fronto-central (Fz, FCz, FC1, FC2), central (Cz), and parieto-occipital (Pz, POz, PO1, PO2) brain regions, along with EMG power spectra for the vastus lateralis muscle, as indicated by the titles. Colors represent cohort-task groups as indicated in the legend. Solid lines indicate the mean power of the active leg, dashed lines indicate the mean power of the passive leg, and shaded areas represent the +/- one standard error (SE). Significant differences between tasks and cohorts at particular frequencies are marked at the top of the plots with dark markers, as depicted by the legend in the EMG subplot. Frequency is plotted on a logarithmic scale. Note that the values are z-scored, making them relative to each other, and, consequently, include negative values.

power was greatest during the dual task; and in the parietooccipital region, the highest peak power occurred during the cognitive task. Across all tasks, the dominant power was observed in the 4–30 Hz range, with prominent peaks in the alpha and high beta bands. However, it is important to note that not all observed qualitative differences were statistically significant.

Statistically significant task-related differences were observed only in the central Cz electrode and parieto-occipital regions. At Cz, power during the cognitive task was significantly lower when compared to the single motor task for frequencies between 4–6 Hz (mean p-value = 0.01) and 29–90 Hz (mean p-value = 0.007) and when compared to the dual task, power was lower for frequencies between 4–17 Hz (mean p-value = 0.003) and 26–90 Hz (mean p-value = 0.006). In the parieto-occipital region, we observed statistically significant differences between motor and cognitive tasks during 7–14 Hz (mean p-value = 0.009).

Statistically significant differences between cohorts were observed exclusively within the gamma frequency ranges. These differences were significant in the fronto-central cluster for all frequencies exceeding 30 Hz (mean p-value = 0.005)

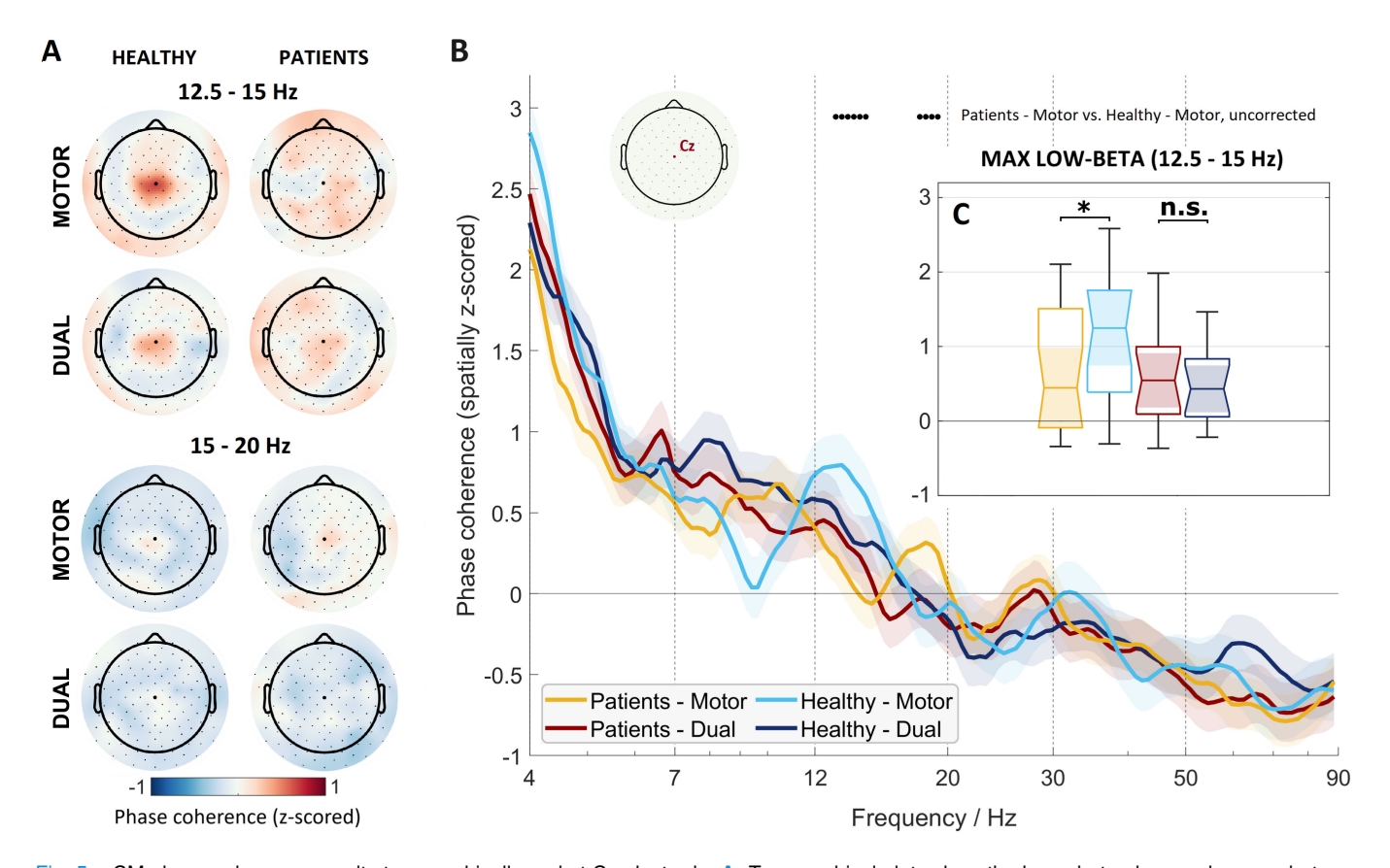


Fig. 5. CM phase coherence results topographically and at Cz electrode. A: Topographical plots show the lower beta phase coherence between the respective scalp electrode and the EMG signal of the active leg. The upper four plots depict phase coherence at 12.5-15 Hz across both cohorts (people with PD / healthy) and tasks (motor / dual). The lower four plots represent CM phase coherence for the same categories but at a 15-20 Hz frequency range. The enlarged dot corresponds to the location of the Cz electrode. B: CM phase coherence of active muscle at Cz electrode across all frequencies (x-axis). Solid lines represent the mean, while the shaded areas represent the +/-1 SE. Significant differences between cohorts for the motor task are marked with black dots at the top of the plots but note that these p-values were uncorrected for multiple comparisons. C: The inset plot shows distributions of maximum low-beta values between 12.5-15 Hz for the four groups, as color-coded by the legend. The abbreviation n.s. indicates a non-significant difference, while the star denotes p < 0.05. Note that the values are z-scored, making them relative to each other, and, consequently, include negative values. Positive phase coherence indicates that the phase coherence for a specific frequency band and electrode position exceeded the average, while negative phase coherence denotes that it was below the average.

and at the Cz electrode, specifically within the narrow frequency range of 35 to 40 Hz (mean p-value = 0.04). People with PD exhibited consistently lower relative power compared to healthy controls.

The EMG frequency spectra for muscle contractions at 30 % MCV peaks between 40–50 Hz (Fig. 4, subfigure EMG). While we observe higher power during the single motor task compared to the dual task, the differences are not statistically significant. Similarly, although the healthy cohort demonstrates higher peak power in both tasks, we do not find statistically significant differences in the peak EMG power spectra. However, we do observe significant differences at frequencies above 82 Hz (mean p-value = 0.04).

B. Cortico-muscular phase coherence

We first present the topographical plots of relative (standardized) CM phase coherence between the EEG electrodes and the averaged EMG for the active muscle in Fig. 5A. The plots show the distribution of CM phase coherence for the low beta-band, separated into frequency ranges of 12.5–15 Hz and 15–20 Hz. We focused on the beta-band, as has been previously documented as an important frequency range for

CM coherence and isometric contraction in general (see Introduction). The topographical plots of other frequency bands are in Appendix VIII (Supplementary Material). Collectively, these plots revealed that the central region around the Cz electrode exhibits the relatively strongest phase coherence with the EMG signal of the active muscle. Based on this observation, we further analyzed the phase coherence at the Cz electrode. Appendix II (Supplementary Material) presents example phase coherence results for two individual participants, while the group analysis is shown in the B and C parts of Fig. 5.

In Fig. 5B, we show CM phase coherence over the frequency spectrum for all four cohort-task groups. By comparing phase coherence values between them, none of the significantly different frequencies survived the multiple comparisons correction. However, we used uncorrected pairwise significant differences between cohorts found in frequency ranges 13–15 Hz and 18–19 Hz (see black dots on top of Fig. 5B) as guiding ranges to extract maximum CM phase coherence values. The reason we decided to also check maximum values over the range, instead of only looking at differences in particular frequencies, is that there is generally a high variability in peak coherence (e.g. see [27], [36], [46], [120], [123]). This

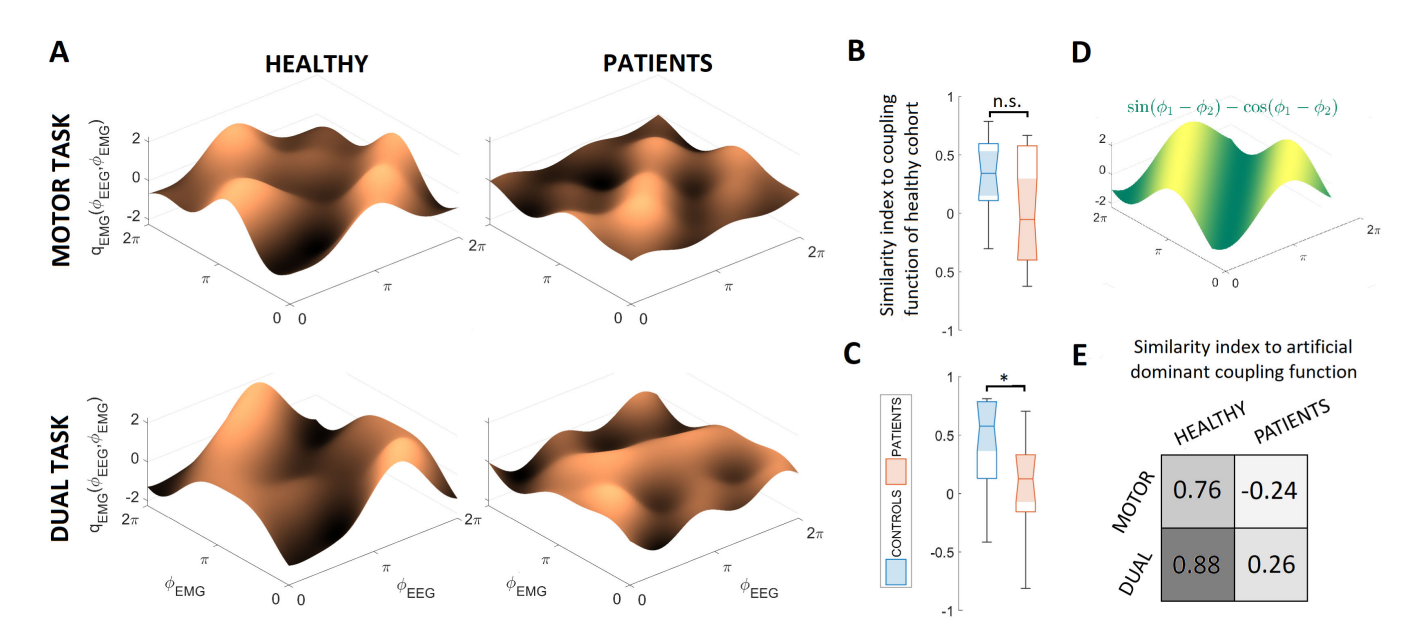


Fig. 6. Inferred coupling functions from the phase dynamics model from EEG Cz electrode to average EMG of the active muscle. A: Median coupling functions, grouped by cohort and task. B: Boxplots show the distributions of similarity indices within cohorts, for the motor task and \mathbb{C} : for the dual task. Distributions are also compared between cohorts, with a star indicating p < 0.05 and n.s. indicating no significant differences. D: Depiction of coupling function with the two dominating terms. E: Matrix showing similarity indices between the dominant coupling function and the median coupling function for each group.

approach thus better accounts for inter-individual differences, as different subjects normally have peak CM phase coherence at different peak frequencies.

We depicted distributions of maximum coherence levels for each cohort-task group with boxplots in inset Fig. 5C. We found significant differences in the main factor task (p =0.031) and significant pairwise differences between people with PD and healthy controls during the single motor task (p = 0.031), in the frequency range of 12.5–15 Hz. No such significant pairwise differences were observed during the dual task (p = 0.74). Additionally, we did not find any significant differences between maximum CM phase coherence in the frequency range of 15-20 Hz (not shown). Given that ztransformation is not commonly employed in this field, we also provide the non-transformed values of phase coherence in Appendix IX (Supplementary Material), where the median was chosen as an aggregating function. The findings are consistent with those obtained after z-transformation. Additionally, in Appendix IX (Supplementary Material) we also present the results for the CM phase coherence between Cz EEG and the EMG of the passive muscle, where, as expected, there were no significant differences between the cohorts or tasks.

C. Phase dynamics modeling

After obtaining a strong beta-band CM phase coherence at the Cz electrode, we modeled the same signals using the phase dynamics model. In this subsection, we present the inferred coupling functions for the four task-cohort groups, and compare their shapes and coupling strengths.

Inferred coupling functions between EEG Cz electrode and average EMG of the active muscle are graphically presented in Fig. 6A.

The coupling function plots are derived by graphing all 24 coupling functions over the period from 0 to 2π , with each function weighted according to the inferred coefficients. If there are no dominant terms, the landscapes appear unstructured; conversely, the plots exhibit discernible structure when dominant terms are present. By visually comparing the median landscapes between the cohorts, a diagonal structure is evident in the healthy cohort during both tasks, which is absent in the patient cohort. To quantitatively compare the coupling functions, we used a similarity index. The results are for the active muscle presented in Fig. 6B for the motor task and in Fig. 6C for the dual task. The analysis revealed that the median similarity index within the healthy cohort for the motor task is 0.34 and 0.58 for the dual task. On the other hand, between the median healthy cohort and individual patients with PD, we observe notably lower median similarity indices (motor task: -0.05, dual task: 0.13). In the motor task, no significant differences between the cohorts were observed. In the dual task, the differences between cohorts were statistically significant (p = 0.046), suggesting that the coupling functions of people with PD differ significantly from those of the healthy cohort.

Furthermore, inferred models for the active muscle are shown in Appendix IX (Supplementary Material). The inferred intrinsic frequencies of the phase oscillators range between 13.6 and 15 Hz, aligning well with the peak levels of the lowbeta CM phase coherence in the healthy cohort. Notably, the models presented only include dominant coupling functions. To identify them, we compared the absolute magnitudes of inferred coefficients to the surrogate distribution, as shown in Appendix X (Supplementary Material). We found two significant dominant coupling terms in the connectivity to the active muscle: $p_{11}\sin(\theta_{emg}-\theta_{eeg})$ and $p_{12}\cos(\theta_{emg}-\theta_{eeg})$,

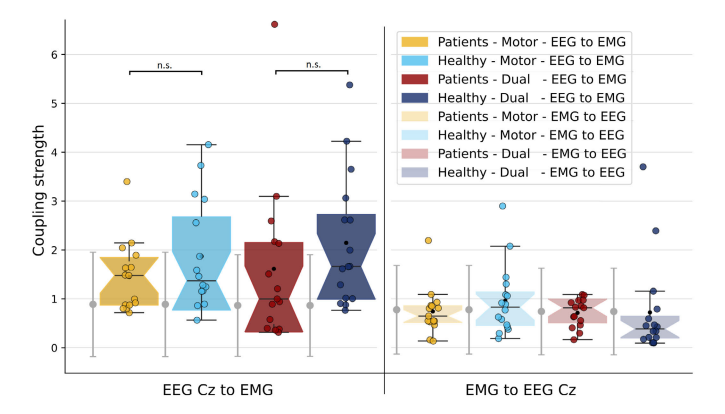


Fig. 7. Phase coupling strength between the Cz EEG electrode and the active muscle. The coupling strength is grouped by the coupling direction (left and right side of the plot) and by cohort and task direction as colour-coded by the legend. Black circles in each distribution correspond to the average value, while the colored dots correspond to the individual participant's values. Grey error bars represent the surrogate average +/-2 SD.

which are plotted in Fig. 6D. The similarity indices between them and the coupling functions of individual groups are shown in Fig. 6E. They are higher in the healthy cohort for both motor ($\rho=0.76$) and dual tasks ($\rho=0.88$). In people with PD, the similarity indices are markedly lower, with $\rho=-0.24$ in the motor and $\rho=0.26$ in the dual task.

Finally, the coupling strength was quantified by calculating the norm of the two coefficients corresponding to the dominant coupling terms. The distributions of coupling strengths for both directions, tasks, and cohorts are shown in Fig. 7. We observed that the strength of coupling from EEG to EMG was significantly greater than in the reverse direction (p = 1.6×10^{-5}), which is to be expected. Further analysis of coupling strengths in the active muscle between cohorts and tasks using the SRH test revealed that the main effect of the task was not significant (p = 0.83), while the main effect of the cohort approached significance (p = 0.056). No significant differences were found when comparing the cohorts for each task individually (motor task: p = 0.34, dual task: p =0.10). However, pairwise comparisons of coupling strength between cohorts, irrespective of the task, showed a significant difference (p = 0.0494), indicating stronger coupling in the healthy cohort.

The phase modeling results between Cz EEG and the EMG of the active muscle, as presented here, are also shown for the passive muscle in Appendix XI (Supplementary Material). In summary, no statistically significant dominant coupling functions were observed in either group, and no significant differences were found between the cohorts.

IV. DISCUSSION

This study investigated cortico-muscular (CM) phase connectivity in early-stage people with Parkinson's disease (PD) and age-matched healthy controls during three tasks: the motor task (isometric knee extension task), the cognitive task (silent serial -3 subtraction task) and the dual task, where both motor and cognitive tasks had to be performed simultaneously. We calculated phase coherence and inferred the phase dynamics

model. The findings of our study are point by point discussed below.

Topographical task-dependent variations in wavelet power spectra outweigh the cohort differences. Our study demonstrates that distinct patterns of rhythmic brain activity emerged across cortical regions under the three task conditions. While these patterns in power spectra were not consistently significant across the entire frequency range, the general pattern remained observable, particularly in the lower frequency ranges up to 20 Hz. In the fronto-central areas, the wavelet power was the lowest during the cognitive task, characterized by minimal motor involvement, and the highest during the motor task, where focused motor actions dominated the participant's attention. During the dual task where participants engaged in both motor and cognitive activities simultaneously, power levels were at an intermediate level. An inverse trend occurred in the parieto-occipital region, where the power up to 20 Hz peaked during the cognitive task, indicating increased cognitive demands. Notably, this region encompasses the intraparietal sulcus (IPS), a critical area involved in arithmetic processing, and number comparison, such as subtraction [124]. These observations align with the dual-task interference concept, which attempts to explain how neural resources are dynamically allocated across cortical regions during multitasking [125], [126], [127], [128].

People with early PD on medications did not show enhanced power in beta band. While we observed the highest peak in the high beta band power (20–30 Hz) in the frontocentral regions during the motor task, it was not significantly higher in comparison to age-matched controls. The absence of elevated power in beta-band, a phenomenon previously reported in people with PD [9], [10], [11], [12], [13], [14], [15], aligns with the characteristics of our cohort, who are receiving medication [17], and are in the early stages of the disease experiencing minimal motor impairment.

EMG power spectrum up to 80 Hz shows no significant variations by task or cohort. Analysis of the EMG power spectra revealed that the healthy cohort exhibited slightly stronger higher frequency activity in the active muscle for both the single motor and the dual task. However, these differences were not statistically significant until frequencies exceeded 80 Hz, a range that is generally less relevant for combined EEG-EMG analysis. Additionally, in people with PD, no resting tremor was observed, which is commonly associated with increased power in the lower frequency range (around 3–6 Hz [129]). This absence can be attributed to the fact that patients were in the early stage of the disease, where tremor symptoms were minimal or absent, as well as to the effects of medications. Furthermore, resting tremors are typically lower in lower limbs and suppressed during voluntary motor activity.

The scalp topography of CM phase coherence differs from the topography of the power spectrum during motor tasks. Phase coherence analysis of the motor tasks revealed that the highest phase coherence in the sensorimotor region occurred above the Cz electrode, almost across the entire frequency spectrum (4–90 Hz). Surprisingly, that region does not overlap with the region of the highest wavelet power during movement, which is the fronto-central region.

To investigate this, we compared our results with two relevant studies [130], [131]. Both studies suggest that there may be greater similarities between the topographical patterns of phase and magnitude-squared CM coherence than between phase coherence and wavelet power. This implies that wavelet power and phase coherence may reflect different aspects of neural activity. While wavelet power might indicate intense processing that occurs independently of muscle connectivity, phase coherence directly reflects the synchronization between motor output in the central motor cortex and muscle activity, as measured by EMG. These results could also be related to seemingly contradictory phenomena: On one hand, beta-band desynchronization is expected in motor areas during movement preparation and execution [132], but in PD, this desynchronization is disinhibited, leading to elevated beta power [9], [10], [11], [12], [13], [14], [15], [16]. On the other hand, high beta-band magnitude-squared coherence between EEG and EMG is typically observed before and during movement [23], [26], [27], [31], [34]. In our study, we observed that both phenomena may exhibit distinct topographies and frequency ranges within the beta band.

Early-stage PD cohort on medication showed differences in CM phase coherence in the lower beta-band (12.5–15 Hz) during the single motor task. We found differences in CM phase coherence already in patients with early-stage PD, who are on anti-parkinsonian medications, which has not been observed previously [13], [133]. The differences were observed in the lower beta-band, specifically between the 12.5 and 15 Hz frequency range, where the healthy cohort showed elevated CM phase coherence, which was not observed in people with PD. The significant difference was not substantial, likely due to high variability among participants and the older age of the control group, who typically also exhibit reduced connectivity due to age-related factors [39], [40], [41], [42], [133], potentially influencing the observed difference in phase coherence as well.

Elevated phase coherence was observed only in the healthy cohort during the single motor task, but not during the dual task, which included a cognitive component. The addition of cognitive tasks requires divided attention, which can impair motor performance, particularly in elderly adults and individuals with movement disorders [134], [135]. Previous research has also shown a reduction in beta-band CM magnitude-squared coherence during dual-task conditions [136], [137]. This reduction has been attributed to the hypothesis that beta-band synchronization in the motor cortex requires focused attention, and decreased attention impairs motor neuron recruitment, a mechanism thought to be underlying the cortical beta-band oscillations [136], [138], [139], [140], [141], [142], [143], [144].

Modeling phase coupling with the phase dynamics model revealed directional asymmetry, showing significantly stronger phase coupling strength from the Cz electrode to the active muscle than vice versa. Despite using different methodologies and examining different muscle groups, our finding aligns with previous studies that employed partial directed coherence [145] and Granger causality [81].

The dominant coupling terms in the phase dynamics model were more pronounced in the healthy than in the patient cohort. We identified two dominant coupling terms that were particularly strong in connectivity to the active muscle: $p_{11} \sin(\theta_{emg} - \theta_{eeg})$ and $p_{12} \cos(\theta_{emg} - \theta_{eeg})$. They represent the sine and cosine components of the phase difference between the EMG and EEG, effectively capturing the phase-locking behavior and reflecting the coupling between cortical and muscular oscillatory activity. The diagonal structure of the coupling function suggests that the coupling is determined by the phase difference between the two oscillators [146]. When the coupling function is positive, the influenced oscillator accelerates, and vice versa when it is negative. Such mechanisms are the basis for synchronization phenomena between the oscillators. As a side note, the fact that the inferred dominant terms include phase difference information supports the use of phase coherence measure as a metric of constant phase difference.

Dominant coupling functions showed qualitatively stronger coupling strength in the healthy cohort compared to the patient cohort, although only marginally significant when the task factor was disregarded. We also observed high variability among participants. Notably, the coupling strength was stronger during the dual task than the single motor task, which is in contrast with the results obtained from phase coherence calculations and something we have to yet better understand.

Neural and behavioral metrics were not significantly correlated. Correlating neural connectivity measures with behavioral outcomes provides insight into the extent to which neurophysiological interactions, measured via EEG and EMG, underlie motor performance. While this has not been previously reported in the paper, we also analyzed the relationship between UPDRS scores and connectivity measures using Spearman correlation, with results presented in Appendix XII (Supplementary Material). We hypothesized a negative correlation between phase connectivity measures and the UPDRS score and observed such a trend for the CM low beta phase coherence during the motor task. The correlations to the dual task and coupling strength of the phase dynamics model were weak or inconsistent. Moreover, none of the correlations were significant. All in all, we think that the UPDRS may not be the optimal behavioral measure, as it relies on subjective scores rather than direct physical measurements, and because all subjects were in the early stage of PD with low scores.

Neurophysiological markers show limited robustness for clinical diagnosis of PD. With this study, we sought to evaluate the potential of CM connectivity measures as neurophysiological markers for clinical practice. Although we did not directly assess this by employing classification models, our observations show significant inter-subject variability. This suggests that the markers may not be robust or reliable enough for general disease classification. However, they could still be valuable for assessing individual improvements in rehabilitation, especially in people exhibiting strong CM phase connectivity.

Limitations of the study. It is important to acknowledge several limitations of the study. The primary limitation is the

low number of trials done by each participant. As the CM connectivity measures are already inherently variable and have high individual differences [36], [46], [120], [123], [147], this even further increased the variance and constrained the assessment of phase connectivity in time. Additionally, we believe this limitation reduced the study's statistical power, preventing some significant differences from surviving correction for multiple comparisons.

Moreover, the study did not account for the delay between EEG and EMG phases when calculating phase coherence or fitting the phase dynamics model. Whereas some studies incorporate delay into the model ([121], [122]) or calculate the delay to assess connectivity direction (e.g. [22]), others do not (e.g. [94]). In our case, we assume the delay is constant, which implies that the phase difference remains stable and should not substantially affect the results. However, this assumption could have introduced a potential source of error.

Lastly, our analysis remained at the surface level of both the brain and muscle. For greater spatial accuracy, it would be more appropriate to directly analyze the time series of dipole-fitted independent components. A similar decomposition could be applied to motor units within the muscle. However, at this initial stage, we chose to remain at the surface level to also explore the potential for clinical applications, which are more straightforward to implement when source analysis is not required.

REFERENCES

- [1] E. Tolosa, C. Gaig, J. Santamaría, and Y. Compta, "Diagnosis and the premotor phase of Parkinson disease," *Neurology*, vol. 72, no. 7, pp. S12–S20, Feb. 2009, doi: 10.1212/wnl.0b013e318198db11.
- [2] J. C. Greenland, C. H. Williams-Gray, and R. A. Barker, "The clinical heterogeneity of Parkinson's disease and its therapeutic implications," *Eur. J. Neurosci.*, vol. 49, no. 3, pp. 328–338, Feb. 2019, doi: 10.1111/ejn.14094.
- [3] H. Braak et al., "Parkinson's disease: Affection of brain stem nuclei controlling premotor and motor neurons of the somatomotor system," *Acta Neuropathologica*, vol. 99, no. 5, pp. 489–495, May 2000, doi: 10.1007/s004010051150.
- [4] Q. Wang, L. Meng, J. Pang, X. Zhu, and D. Ming, "Characterization of EEG data revealing relationships with cognitive and motor symptoms in Parkinson's disease: A systematic review," *Frontiers Aging Neurosci.*, vol. 12, Nov. 2020, Art. no. 587396, doi: 10.3389/fnagi.2020.587396.
- [5] C. H. Hawkes, K. Del Tredici, and H. Braak, "Parkinson's disease: A dual-hit hypothesis," *Neuropathol. Appl. Neurobiol.*, vol. 33, no. 6, pp. 599–614, Dec. 2007, doi: 10.1111/j.1365-2990.2007.00874.x.
- [6] E. Tolosa, A. Garrido, S. Scholz, and W. Poewe, "Challenges in the diagnosis of Parkinson's disease," *Lancet Neurol.*, vol. 20, no. 5, pp. 385–397, 2021, doi: 10.1016/S1474-4422(21)00030-2.
- [7] H. Braak, K. D. Tredici, U. Rüb, R. A. I. de Vos, E. N. H. Jansen Steur, and E. Braak, "Staging of brain pathology related to sporadic Parkinson's disease," *Neurobiol. Aging*, vol. 24, no. 2, pp. 197–211, Mar. 2003, doi: 10.1016/s0197-4580(02)00065-9.
- [8] E. Tolosa, G. Wenning, and W. Poewe, "The diagnosis of Parkinson's disease," *Lancet Neurol.*, vol. 5, no. 1, pp. 75–86, Jan. 2006, doi: 10.1016/s1474-4422(05)70285-4.
- [9] P. Brown, "Oscillatory nature of human basal ganglia activity: Relationship to the pathophysiology of Parkinson's disease," *Movement Disorders*, vol. 18, no. 4, pp. 357–363, Apr. 2003, doi: 10.1002/mds.10358.
- [10] W. D. Hutchison et al., "Neuronal oscillations in the basal ganglia and movement disorders: Evidence from whole animal and human recordings: Figure 1," *J. Neurosci.*, vol. 24, no. 42, pp. 9240–9243, Oct. 2004, doi: 10.1523/jneurosci.3366-04.2004.
- [11] A. Schnitzler and J. Gross, "Normal and pathological oscillatory communication in the brain," *Nature Rev. Neurosci.*, vol. 6, no. 4, pp. 285–296, Apr. 2005, doi: 10.1038/nrn1650.

- [12] H. W. Berendse and C. J. Stam, "Stage-dependent patterns of disturbed neural synchrony in Parkinson's disease," *Parkinsonism Rel. Disorders*, vol. 13, pp. S440–S445, 2007, doi: 10.1016/s1353-8020(08)70046-4.
- [13] B. Pollok, V. Krause, W. Martsch, C. Wach, A. Schnitzler, and M. Südmeyer, "Motor-cortical oscillations in early stages of Parkinson's disease," *J. Physiol.*, vol. 590, no. 13, pp. 3203–3212, Jul. 2012, doi: 10.1113/jphysiol.2012.231316.
- [14] E. Stein and I. Bar-Gad, "Beta oscillations in the cortico-basal ganglia loop during parkinsonism," *Experim. Neurol.*, vol. 245, pp. 52–59, Jul. 2013, doi: 10.1016/j.expneurol.2012.07.023.
- [15] A. Oswal, P. Brown, and V. Litvak, "Synchronized neural oscillations and the pathophysiology of Parkinson's disease," *Current Opinion Neurol.*, vol. 26, no. 6, pp. 662–670, Dec. 2013, doi: 10.1097/wco.0000000000000034.
- [16] A. Singh, R. C. Cole, A. I. Espinoza, D. Brown, J. F. Cavanagh, and N. S. Narayanan, "Frontal theta and beta oscillations during lower-limb movement in Parkinson's disease," *Clin. Neurophysiol.*, vol. 131, no. 3, pp. 694–702, Mar. 2020, doi: 10.1016/j.clinph.2019.12.399.
- [17] P. Brown and C. D. Marsden, "Bradykinesia and impairment of EEG desynchronization in Parkinson's disease," *Mov. Disord.*, vol. 14, no. 3, pp. 423–429, May 1999, doi: 10.1002/1531-8257(199905)14:3<423::AID-MDS1006>3.0.CO;2-V.
- [18] P. Silberstein et al., "Cortico-cortical coupling in Parkinson's disease and its modulation by therapy," *Brain*, vol. 128, no. 6, pp. 1277–1291, Jun. 2005, doi: 10.1093/brain/awh480.
- [19] S. R. Cole, R. van der Meij, E. J. Peterson, C. de Hemptinne, P. A. Starr, and B. Voytek, "Nonsinusoidal beta oscillations reflect cortical pathophysiology in Parkinson's disease," *J. Neurosci.*, vol. 37, no. 18, pp. 4830–4840, May 2017, doi: 10.1523/jneurosci.2208-16.2017.
- [20] Z. D. Zhou, L. X. Yi, D. Q. Wang, T. M. Lim, and E. K. Tan, "Role of dopamine in the pathophysiology of Parkinson's disease," *Transl. Neurodegeneration*, vol. 12, no. 1, p. 44, Sep. 2023, doi: 10.1186/s40035-023-00378-6.
- [21] M. J. Armstrong and M. S. Okun, "Diagnosis and treatment of Parkinson disease: A review," *Jama*, vol. 323, no. 6, pp. 548–560, Feb. 2020, doi: 10.1001/jama.2019.22360.
- [22] T. Mima and M. Hallett, "Corticomuscular coherence: A review," J. Clin. Neurophysiol. Off. Publication Amer. Electroencephalogr. Soc., vol. 16, no. 6, pp. 501–511, Nov. 1999, doi: 10.1097/00004691-199911000-00002.
- [23] J. Liu, Y. Sheng, and H. Liu, "Corticomuscular coherence and its applications: A review," Frontiers Hum. Neurosci., vol. 13, p. 100, Mar. 2019, doi: 10.3389/fnhum.2019.00100.
- [24] P. L. Nunez et al., "EEG coherency," *Electroencephalogr. Clin. Neuro-physiol.*, vol. 103, no. 5, pp. 499–515, Nov. 1997, doi: 10.1016/s0013-4694(97)00066-7.
- [25] J.-P. Lachaux et al., "Estimating the time-course of coherence between single-trial brain signals: An introduction to wavelet coherence," *Neu-rophysiologie Clinique/Clin. Neurophysiol.*, vol. 32, no. 3, pp. 157–174, Jun. 2002, doi: 10.1016/s0987-7053(02)00301-5.
- [26] S. N. Baker, E. Olivier, and R. N. Lemon, "Coherent oscillations in monkey motor cortex and hand muscle EMG show task-dependent modulation," *J. Physiol.*, vol. 501, no. 1, pp. 225–241, May 1997, doi: 10.1111/j.1469-7793.1997.225bo.x.
- [27] B. A. Conway et al., "Synchronization between motor cortex and spinal motoneuronal pool during the performance of a maintained motor task in man," *J. Physiol.*, vol. 489, no. 3, pp. 917–924, Dec. 1995, doi: 10.1113/jphysiol.1995.sp021104.
- [28] S. F. Farmer, F. D. Bremner, D. M. Halliday, J. R. Rosenberg, and J. A. Stephens, "The frequency content of common synaptic inputs to motoneurones studied during voluntary isometric contraction in man," *J. Physiol.*, vol. 470, no. 1, pp. 127–155, Oct. 1993, doi: 10.1113/jphysiol.1993.sp019851.
- [29] D. M. Halliday, B. A. Conway, S. F. Farmer, and J. R. Rosenberg, "Using electroencephalography to study functional coupling between cortical activity and electromyograms during voluntary contractions in humans," *Neurosci. Lett.*, vol. 241, no. 1, pp. 5–8, Jan. 1998, doi: 10.1016/s0304-3940(97)00964-6.
- [30] S. Salenius and R. Hari, "Synchronous cortical oscillatory activity during motor action," *Current Opinion Neurobiol.*, vol. 13, no. 6, pp. 678–684, Dec. 2003, doi: 10.1016/j.conb.2003.10.008.
- [31] A. Andrykiewicz, L. Patino, J. R. Naranjo, M. Witte, M.-C. Hepp-Reymond, and R. Kristeva, "Corticomuscular synchronization with small and large dynamic force output," *BMC Neurosci.*, vol. 8, no. 1, p. 101, Nov. 2007, doi: 10.1186/1471-2202-8-101.

- [32] X. Xi, X. Wu, Y.-B. Zhao, J. Wang, W. Kong, and Z. Luo, "Cortico-muscular functional network: An exploration of cortico-muscular coupling in hand movements," *J. Neural Eng.*, vol. 18, no. 4, Jun. 2021, Art. no. 046084, doi: 10.1088/1741-2552/ac0586.
- [33] M. Fauvet, D. Gasq, A. Chalard, J. Tisseyre, and D. Amarantini, "Temporal dynamics of corticomuscular coherence reflects alteration of the central mechanisms of neural motor control in post-stroke patients," *Frontiers Hum. Neurosci.*, vol. 15, Jul. 2021, Art. no. 682080, doi: 10.3389/fnhum.2021.682080.
- [34] L. Zhou et al., "Cortico-muscular coherence of time-frequency and spatial characteristics under movement observation, movement execution, and movement imagery," *Cogn. Neurodyn.*, vol. 18, no. 3, pp. 1079–1096, Apr. 2023.
- [35] R. Kristeva, L. Patino, and W. Omlor, "Beta-range cortical motor spectral power and corticomuscular coherence as a mechanism for effective corticospinal interaction during steady-state motor output," *NeuroImage*, vol. 36, no. 3, pp. 785–792, Jul. 2007, doi: 10.1016/j.neuroimage.2007.03.025.
- [36] I. Mendez-Balbuena, F. Huethe, J. Schulte-Monting, R. Leonhart, E. Manjarrez, and R. Kristeva, "Corticomuscular coherence reflects interindividual differences in the state of the corticomuscular network during low-level static and dynamic forces," *Cerebral Cortex*, vol. 22, no. 3, pp. 628–638, Mar. 2012, doi: 10.1093/cercor/bhr147.
- [37] M. A. Perez, J. Lundbye-Jensen, and J. B. Nielsen, "Changes in corticospinal drive to spinal motoneurones following visuo-motor skill learning in humans," *J. Physiol.*, vol. 573, no. 3, pp. 843–855, Jun. 2006, doi: 10.1113/jphysiol.2006.105361.
- [38] T. Yamaguchi et al., "Transcranial alternating current stimulation of the primary motor cortex after skill acquisition improves motor memory retention in humans: A double-blinded sham-controlled study," *Cerebral Cortex Commun.*, vol. 1, no. 1, Aug. 2020, Art. no. tgaa047, doi: 10.1093/texcom/tgaa047.
- [39] A. N. Johnson and M. Shinohara, "Corticomuscular coherence with and without additional task in the elderly," J. Appl. Physiol., vol. 112, no. 6, pp. 970–981, Mar. 2012, doi: 10.1152/japplphysiol.01079.2011.
- [40] M. B. Bayram, V. Siemionow, and G. H. Yue, "Weakening of corticomuscular signal coupling during voluntary motor action in aging," J. Gerontol. A, Biol. Sci. Med. Sci., vol. 70, no. 8, pp. 1037–1043, Mar. 2015, doi: 10.1093/gerona/glv014.
- [41] D. Kamp, V. Krause, M. Butz, A. Schnitzler, and B. Pollok, "Changes of cortico-muscular coherence: An early marker of healthy aging?" AGE, vol. 35, no. 1, pp. 49–58, Feb. 2013, doi: 10.1007/s11357-011-9329-y.
- [42] M. E. Spedden, J. B. Nielsen, and S. S. Geertsen, "Oscillatory corticospinal activity during static contraction of ankle muscles is reduced in healthy old versus young adults," *Neural Plasticity*, vol. 2018, pp. 1–13, Jan. 2018, doi: 10.1155/2018/3432649.
- [43] T. Mima, K. Toma, B. Koshy, and M. Hallett, "Coherence between cortical and muscular activities after subcortical stroke," *Stroke*, vol. 32, no. 11, pp. 2597–2601, Nov. 2001, doi: 10.1161/hs1101.098764.
- [44] Y. Fang et al., "Functional corticomuscular connection during reaching is weakened following stroke," *Clin. Neurophysiol.*, vol. 120, no. 5, pp. 994–1002, May 2009, doi: 10.1016/j.clinph.2009.02.173.
- [45] K. von Carlowitz-Ghori, Z. Bayraktaroglu, F. U. Hohlefeld, F. Losch, G. Curio, and V. V. Nikulin, "Corticomuscular coherence in acute and chronic stroke," *Clin. Neurophysiol. Off. J. Int. Fed. Clin. Neurophysiol.*, vol. 125, no. 6, pp. 1182–1191, Jun. 2014, doi: 10.1016/j.clinph.2013.11.006.
- [46] P. Belardinelli, L. Laer, E. Ortiz, C. Braun, and A. Gharabaghi, "Plasticity of premotor cortico-muscular coherence in severely impaired stroke patients with hand paralysis," *NeuroImage, Clin.*, vol. 14, pp. 726–733, Jan. 2017, doi: 10.1016/j.nicl.2017.03.005.
- [47] R. Aikio et al., "CMC is more than a measure of corticospinal tract integrity in acute stroke patients," *NeuroImage, Clin.*, vol. 32, Jan. 2021, Art. no. 102818, doi: 10.1016/j.nicl.2021.102818.
- [48] M. Proudfoot et al., "Impaired corticomuscular and interhemispheric cortical beta oscillation coupling in amyotrophic lateral sclerosis," *Clin. Neurophysiol.*, vol. 129, no. 7, pp. 1479–1489, Jul. 2018, doi: 10.1016/j.clinph.2018.03.019.
- [49] K. M. Fisher, B. Zaaimi, T. L. Williams, S. N. Baker, and M. R. Baker, "Beta-band intermuscular coherence: A novel biomarker of upper motor neuron dysfunction in motor neuron disease," *Brain*, vol. 135, no. 9, pp. 2849–2864, Sep. 2012, doi: 10.1093/brain/aws150.

- [50] M. Padalino et al., "Effects on motor control of personalized neuromodulation against multiple sclerosis fatigue," *Brain Topography*, vol. 34, no. 3, pp. 363–372, May 2021, doi: 10.1007/s10548-021-00820-w.
- [51] H. Park, J. S. Kim, S. H. Paek, B. S. Jeon, J. Y. Lee, and C. K. Chung, "Cortico-muscular coherence increases with tremor improvement after deep brain stimulation in Parkinson's disease," *NeuroReport*, vol. 20, no. 16, pp. 1444–1449, Oct. 2009, doi: 10.1097/wnr.0b013e328331a51a.
- [52] D. Weiss et al., "Subthalamic nucleus stimulation restores the efferent cortical drive to muscle in parallel to functional motor improvement," *Eur. J. Neurosci.*, vol. 35, no. 6, pp. 896–908, Mar. 2012, doi: 10.1111/j.1460-9568.2012.08014.x.
- [53] N. Zokaei, A. J. Quinn, M. T. Hu, M. Husain, F. van Ede, and A. C. Nobre, "Reduced cortico-muscular beta coupling in Parkinson's disease predicts motor impairment," *Brain Commun.*, vol. 3, no. 3, Aug. 2021, Art. no. fcab179, doi: 10.1093/braincomms/fcab179.
- [54] B. A. Conway, D. M. Halliday, and J. R. Rosenberg, "Rhythmic cortical activity and its relation to the neurogenic components of normal and pathological tremors," *Prog. Brain Res.*, vol. 123, pp. 437–444, 1999, doi: 10.1016/S0079-6123(08)62879-4.
- [55] B. Hellwig et al., "Tremor-correlated cortical activity detected by electroencephalography," Clin. Neurophysiol., vol. 111, no. 5, pp. 806–809, May 2000, doi: 10.1016/s1388-2457(00)00248-0.
- [56] A. Schnitzler, L. Timmermann, and J. Gross, "Physiological and pathological oscillatory networks in the human motor system," *J. Physiology-Paris*, vol. 99, no. 1, pp. 3–7, Jan. 2006, doi: 10.1016/j.jphysparis.2005.06.010.
- [57] J. N. Caviness, C. H. Adler, M. N. Sabbagh, D. J. Connor, J. L. Hernandez, and T. D. Lagerlund, "Abnormal corticomuscular coherence is associated with the small amplitude cortical myoclonus in Parkinson's disease," *Movement Disorders*, vol. 18, no. 10, pp. 1157–1162, Oct. 2003, doi: 10.1002/mds.10525.
- [58] J. N. Caviness, H. A. Shill, M. N. Sabbagh, V. G. H. Evidente, J. L. Hernandez, and C. H. Adler, "Corticomuscular coherence is increased in the small postural tremor of Parkinson's disease," *Movement Disorders*, vol. 21, no. 4, pp. 492–499, Apr. 2006, doi: 10.1002/mds.20743.
- [59] Y. Yang, J. P. A. Dewald, F. C. T. van der Helm, and A. C. Schouten, "Unveiling neural coupling within the sensorimotor system: Directionality and nonlinearity," *Eur. J. Neurosci.*, vol. 48, no. 7, pp. 2407–2415, Oct. 2018, doi: 10.1111/ejn.13692.
- [60] G. B. Ermentrout, "N: M phase-locking of weakly coupled oscillators," J. Math. Biol., vol. 12, no. 3, pp. 327–342, Aug. 1981, doi: 10.1007/bf00276920.
- [61] J. P. Lachaux, E. Rodriguez, J. Martinerie, and F. J. Varela, "Measuring phase synchrony in brain signals," *Hum. Brain Mapping*, vol. 8, no. 4, pp. 194–208, Jan. 1999, doi: 10.1002/(SICI)1097-0193(1999)8:4<194::AID-HBM4>3.0.CO;2-C.
- [62] A. Bandrivskyy, A. Bernjak, P. McClintock, and A. Stefanovska, "Wavelet phase coherence analysis: Application to skin temperature and blood flow," *Cardiovascular Eng.*, vol. 4, no. 1, pp. 89–93, Mar. 2004.
- [63] M. J. Kaminski and K. J. Blinowska, "A new method of the description of the information flow in the brain structures," *Biol. Cybern.*, vol. 65, no. 3, pp. 203–210, Jul. 1991, doi: 10.1007/bf00198091.
- [64] F. Artoni et al., "Unidirectional brain to muscle connectivity reveals motor cortex control of leg muscles during stereotyped walking," *NeuroImage*, vol. 159, pp. 403–416, Oct. 2017, doi: 10.1016/j.neuroimage.2017.07.013.
- [65] L. A. Baccalá and K. Sameshima, "Partial directed coherence: A new concept in neural structure determination," *Biol. Cybern.*, vol. 84, no. 6, pp. 463–474, May 2001, doi: 10.1007/PL00007990.
- [66] V. Youssofzadeh, D. Zanotto, K. Wong-Lin, S. K. Agrawal, and G. Prasad, "Directed functional connectivity in fronto-centroparietal circuit correlates with motor adaptation in gait training," *IEEE Trans. Neural Syst. Rehabil. Eng.*, vol. 24, no. 11, pp. 1265–1275, Nov. 2016, doi: 10.1109/TNSRE.2016.2551642.
- [67] F. He, S. A. Billings, H.-L. Wei, and P. G. Sarrigiannis, "A nonlinear causality measure in the frequency domain: Nonlinear partial directed coherence with applications to EEG," *J. Neurosci. Methods*, vol. 225, pp. 71–80, Mar. 2014, doi: 10.1016/j.jneumeth.2014.01.013.
- [68] R. Vicente, M. Wibral, M. Lindner, and G. Pipa, "Transfer entropy—A model-free measure of effective connectivity for the neurosciences," *J. Comput. Neurosci.*, vol. 30, no. 1, pp. 45–67, Feb. 2011, doi: 10.1007/s10827-010-0262-3.

- [69] H. Hinrichs, T. Noesselt, and H. Heinze, "Directed information flow—A model free measure to analyze causal interactions in event related EEG-MEG-experiments," *Human Brain Mapping*, vol. 29, no. 2, pp. 193–206, Feb. 2008, doi: 10.1002/hbm.20382.
- [70] X. Chen, Y. Zhang, S. Cheng, and P. Xie, "Transfer spectral entropy and application to functional corticomuscular coupling," *IEEE Trans. Neural Syst. Rehabil. Eng.*, vol. 27, no. 5, pp. 1092–1102, May 2019, doi: 10.1109/TNSRE.2019.2907148.
- [71] Z. Zhang, S. Sun, M. Yi, X. Wu, and Y. Ding, "MIC as an appropriate method to construct the brain functional network," *BioMed Res. Int.*, vol. 2015, pp. 1–10, Jan. 2015, doi: 10.1155/2015/825136.
- [72] T. Liang, Q. Zhang, X. Liu, C. Lou, X. Liu, and H. Wang, "Time-frequency maximal information coefficient method and its application to functional corticomuscular coupling," *IEEE Trans. Neural Syst. Rehabil. Eng.*, vol. 28, no. 11, pp. 2515–2524, Nov. 2020, doi: 10.1109/TNSRE.2020.3028199.
- [73] K. J. Friston, L. Harrison, and W. Penny, "Dynamic causal modeling," *NeuroImage*, vol. 19, no. 4, pp. 1273–1302, Aug. 2003, doi: 10.1016/s1053-8119(03)00202-7.
- [74] V. N. Smelyanskiy, D. G. Luchinsky, A. Stefanovska, and P. V. E. McClintock, "Inference of a nonlinear stochastic model of the cardiorespiratory interaction," *Phys. Rev. Lett.*, vol. 94, no. 9, Mar. 2005, Art. no. 098101, doi: 10.1103/physrevlett.94.098101.
- [75] T. Stankovski, A. Duggento, P. V. E. McClintock, and A. Stefanovska, "Inference of time-evolving coupled dynamical systems in the presence of noise," *Phys. Rev. Lett.*, vol. 109, no. 2, Jul. 2012, Art. no. 024101, doi: 10.1103/physrevlett.109.024101.
- [76] T. Stankovski, A. Duggento, P. V. E. McClintock, and A. Stefanovska, "A tutorial on time-evolving dynamical Bayesian inference," *Eur. Phys. J. Special Topics*, vol. 223, no. 13, pp. 2685–2703, Dec. 2014, doi: 10.1140/epjst/e2014-02286-7.
- [77] P. Sauseng and W. Klimesch, "What does phase information of oscillatory brain activity tell us about cognitive processes?" *Neurosci. Biobehavioral Rev.*, vol. 32, no. 5, pp. 1001–1013, Jul. 2008, doi: 10.1016/j.neubiorev.2008.03.014.
- [78] S. J. K. Barnes, J. Bjerkan, P. T. Clemson, J. Newman, and A. Stefanovska, "Phase coherence—A time-localized approach to studying interactions," *Chaos, Interdiscipl. J. Nonlinear Sci.*, vol. 34, no. 7, Jul. 2024, Art. no. 073155, doi: 10.1063/5.0202865.
- [79] A. K. Engel, P. Fries, and W. Singer, "Dynamic predictions: Oscillations and synchrony in top-down processing," *Nature Rev. Neurosci.*, vol. 2, no. 10, pp. 704–716, Oct. 2001, doi: 10.1038/35094565.
- [80] T. Womelsdorf and P. Fries, "Neuronal coherence during selective attentional processing and sensory-motor integration," *J. Physiol.-Paris*, vol. 100, no. 4, pp. 182–193, Oct. 2006, doi: 10.1016/j.jphysparis.2007.01.005.
- [81] A. Tomassini, E. Maris, P. Hilt, L. Fadiga, and A. D'Ausilio, "Visual detection is locked to the internal dynamics of cortico-motor control," *PLOS Biol.*, vol. 18, no. 10, Oct. 2020, Art. no. e3000898, doi: 10.1371/journal.pbio.3000898.
- [82] E. Maris, P. Fries, and F. van Ede, "Diverse phase relations among neuronal rhythms and their potential function," *Trends Neurosci.*, vol. 39, no. 2, pp. 86–99, Feb. 2016, doi: 10.1016/j.tins.2015.12.004.
- [83] T. Mima, J. Steger, A. E. Schulman, C. Gerloff, and M. Hallett, "Electroencephalographic measurement of motor cortex control of muscle activity in humans," *Clin. Neurophysiol.*, vol. 111, no. 2, pp. 326–337, Feb. 2000, doi: 10.1016/s1388-2457(99)00229-1.
- [84] J. Raethjen et al., "Corticomuscular coherence in the 6–15 Hz band: Is the cortex involved in the generation of physiologic tremor?" Exp. Brain Res., vol. 142, no. 1, pp. 32–40, Jan. 2002, doi: 10.1007/s00221-001-0914-7.
- [85] S. Mehrkanoon, M. Breakspear, and T. W. Boonstra, "The reorganization of corticomuscular coherence during a transition between sensorimotor states," *NeuroImage*, vol. 100, pp. 692–702, Oct. 2014, doi: 10.1016/j.neuroimage.2014.06.050.
- [86] Y. Yang, T. Solis-Escalante, J. Yao, A. Daffertshofer, A. C. Schouten, and F. C. T. van der Helm, "A general approach for quantifying nonlinear connectivity in the nervous system based on phase coupling," *Int. J. Neural Syst.*, vol. 26, no. 1, Feb. 2016, Art. no. 1550031, doi: 10.1142/s0129065715500318.
- [87] N. Parmar, P. Sirpal, W. A. Sikora, J. P. A. Dewald, H. H. Refai, and Y. Yang, "Beta-band cortico-muscular phase coherence in hemi-paretic stroke," *Biomed. Signal Process. Control*, vol. 97, Nov. 2024, Art. no. 106719, doi: 10.1016/j.bspc.2024.106719.

- [88] Y. Kuramoto, "Self-entrainment of a population of coupled non-linear oscillators," in *Proc. Int. Symp. Math. Problems Theor. Phys.* Cham, Switzerland: Springer, 1975, pp. 420–422, doi: 10.1007/BFb0013365.
- [89] J. A. Acebrón, L. L. Bonilla, C. J. P. Vicente, F. Ritort, and R. Spigler, "The Kuramoto model: A simple paradigm for synchronization phenomena," *Rev. Mod. Phys.*, vol. 77, no. 1, pp. 137–185, Apr. 2005, doi: 10.1103/revmodphys.77.137.
- [90] K. J. Friston, "Functional and effective connectivity: A review," *Brain Connectivity*, vol. 1, no. 1, pp. 13–36, Jan. 2011, doi: 10.1089/brain.2011.0008.
- [91] T. Stankovski, V. Ticcinelli, P. V. E. McClintock, and A. Stefanovska, "Neural cross-frequency coupling functions," *Frontiers Syst. Neurosci.*, vol. 11, p. 33, Jun. 2017, doi: 10.3389/fnsys.2017.00033.
- [92] T. Stankovski, T. Pereira, P. V. E. McClintock, and A. Stefanovska, "Coupling functions: Universal insights into dynamical interaction mechanisms," *Rev. Modern Phys.*, vol. 89, no. 4, Nov. 2017, Art. no. 045001, doi: 10.1103/revmodphys.89.045001.
- [93] Z. Sverko, J. Sajovic, G. Drevensek, S. Vlahinic, and P. Rogelj, "Generation of oscillatory synthetic signal simulating brain network dynamics," in *Proc. 44th Int. Conv. Inf., Commun. Electron. Technol. (MIPRO)*, Sep. 2021, pp. 141–146, doi: 10.23919/mipro52101.2021.9597039.
- [94] D. Manasova and T. Stankovski, "Neural cross-frequency coupling functions in sleep," *Neuroscience*, vol. 523, pp. 20–30, Jul. 2023, doi: 10.1016/j.neuroscience.2023.05.016.
- [95] D. Lukarski, S. Petkoski, P. Ji, and T. Stankovski, "Delta-alpha cross-frequency coupling for different brain regions," *Chaos: Interdiscipl. J. Nonlinear Sci.*, vol. 33, no. 10, Oct. 2023, Art. no. 103126, doi: 10.1063/5.0157979.
- [96] A. Mirelman et al., "Increased frontal brain activation during walking while dual tasking: An fNIRS study in healthy young adults," J. NeuroEng. Rehabil., vol. 11, pp. 1–7, 2014, doi: 10.1186/1743-0003-11-85.
- [97] H. Ohsugi, S. Ohgi, K. Shigemori, and E. B. Schneider, "Differences in dual-task performance and prefrontal cortex activation between younger and older adults," *BMC Neurosci.*, vol. 14, pp. 1–9, 2013, doi: 10.1186/1471-2202-14-10.
- [98] J. Benito-Le et al., "Tremor severity in Parkinson's disease and cortical changes of areas controlling movement sequencing: A preliminary study," J. Neurosci. Res., vol. 96, no. 8, pp. 1341–1352, 2018, doi: 10.1002/jnr.24248.
- [99] C. G. Goetz et al., "Movement disorder society-sponsored revision of the unified Parkinson's disease rating scale (MDS-UPDRS): Scale presentation and clinimetric testing results," *Movement Disorders, Off. J. Movement Disorder Soc.*, vol. 23, no. 15, pp. 2129–2170, 2008, doi: 10.1002/mds.22340.
- [100] U. Marusic, M. Peskar, M. M. Šömen, M. Kalc, A. Holobar, and K. Gramann, "Neuromuscular assessment of force development, postural, and gait performance under cognitive-motor dual-tasking in healthy older adults and people with early Parkinson's disease: Study protocol for a cross-sectional mobile brain/body imaging (MoBI) study," *Open Res. Eur.*, vol. 3, 2023.
- [101] R. Oostenveld and P. Praamstra, "The five percent electrode system for high-resolution EEG and ERP measurements," *Clin. Neuro-physiol.*, vol. 112, no. 4, pp. 713–719, 2001, doi: 10.1016/S1388-2457(00)00527-7.
- [102] A. Delorme and S. Makeig, "EEGLAB: An open source toolbox for analysis of single-trial EEG dynamics including independent component analysis," *J. Neurosci. Methods*, vol. 134, no. 1, pp. 9–21, Mar. 2004, doi: 10.1016/j.jneumeth.2003.10.009.
- [103] J. Newman, G. Lancaster, and A. Stefanovska. (Sep. 2018). Multiscale Oscillatory Dynamics Analysis V1.01: User Manual. [Online]. Available: https://www.matrix-inst.org.au/wp_Matrix2016/wp-content/uploads/2019/2019_07_Angelova/MODA-User-Manual.pdf
- [104] A. de Cheveigné, "ZapLine: A simple and effective method to remove power line artifacts," *NeuroImage*, vol. 207, Feb. 2020, Art. no. 116356, doi: 10.1016/j.neuroimage.2019.116356.
- [105] M. Klug and N. A. Kloosterman, "Zapline-plus: A zapline extension for automatic and adaptive removal of frequency-specific noise artifacts in M/EEG," *Human Brain Mapping*, vol. 43, no. 9, pp. 2743–2758, Jun. 2022, doi: 10.1002/hbm.25832.
- [106] L. Pion-Tonachini, K. Kreutz-Delgado, and S. Makeig, "ICLabel: An automated electroencephalographic independent component classifier, dataset, and website," *NeuroImage*, vol. 198, pp. 181–197, Sep. 2019, doi: 10.1016/j.neuroimage.2019.05.026.

- [107] R. Oostenveld, P. Praamstra, D. F. Stegeman, and A. van Oosterom, "Overlap of attention and movement-related activity in lateralized event-related brain potentials," *Clin. Neurophysiol.*, vol. 112, no. 3, pp. 477–484, Mar. 2001, doi: 10.1016/s1388-2457(01)00460-6.
- [108] J. Bigot, M. Longcamp, F. Dal Maso, and D. Amarantini, "A new statistical test based on the wavelet cross-spectrum to detect time-frequency dependence between non-stationary signals: Application to the analysis of cortico-muscular interactions," *NeuroImage*, vol. 55, no. 4, pp. 1504–1518, Apr. 2011, doi: 10.1016/j.neuroimage.2011.01.033.
- [109] V. M. McClelland, Z. Cvetkovic, and K. R. Mills, "Rectification of the EMG is an unnecessary and inappropriate step in the calculation of corticomuscular coherence," *J. Neurosci. Methods*, vol. 205, no. 1, pp. 190–201, Mar. 2012, doi: 10.1016/j.jneumeth.2011.11.001.
- [110] Y. Ruiz-Gonzalez, L. Velázquez-Pérez, R. Rodríguez-Labrada, R. Torres-Vega, and U. Ziemann, "ole of EMG rectification for corticomuscular and intermuscular coherence estimation of spinocerebellar ataxia type 2 (SCA2)," in *Proc. 24th Iberoamerican Congr.* Cham, Switzerland: Springer, 2019, pp. 306–315, doi: 10.1007/978-3-030-33904-3 28.
- [111] W. Penfield and E. Boldrey, "Somatic motor and sensory representation in the cerebral cortex of man as studied by electrical stimulation," *Brain*, vol. 60, no. 4, pp. 389–443, 1937, doi: 10.1093/brain/60.4.389.
- [112] C. J. Scheirer, W. S. Ray, and N. Hare, "The analysis of ranked data derived from completely randomized factorial designs," *Biometrics*, vol. 32, no. 2, p. 429, Jun. 1976, doi: 10.2307/2529511.
- [113] Y. Benjamini and Y. Hochberg, "Controlling the false discovery rate: A practical and powerful approach to multiple testing," *J. Roy. Stat. Soc.*, *B*, vol. 57, no. 1, pp. 289–300, Jan. 1995, doi: 10.1111/j.2517-6161.1995.tb02031.x.
- [114] F. Mormann, K. Lehnertz, P. David, and C. E. Elger, "Mean phase coherence as a measure for phase synchronization and its application to the EEG of epilepsy patients," *Phys. D, Nonlinear Phenomena*, vol. 144, nos. 3–4, pp. 358–369, Oct. 2000, doi: 10.1016/S0167-2789(00)00087-7.
- [115] F. Wilcoxon, "Individual comparisons by ranking methods," in Breakthroughs in Statistics: Methodology and Distribution. Cham, Switzerland: Springer, 1992, pp. 196–202, doi: 10.1007/978-1-4612-4380-9_16.
- [116] G. Lancaster, D. Iatsenko, A. Pidde, V. Ticcinelli, and A. Stefanovska, "Surrogate data for hypothesis testing of physical systems," *Phys. Rep.*, vol. 748, pp. 1–60, Jul. 2018, doi: 10.1016/j.physrep.2018.06.001.
- [117] B. Kralemann, L. Cimponeriu, M. Rosenblum, A. Pikovsky, and R. Mrowka, "Phase dynamics of coupled oscillators reconstructed from data," *Phys. Rev. E, Stat. Phys. Plasmas Fluids Relat. Interdiscip. Top.*, vol. 77, no. 6, Jun. 2008, Art. no. 066205, doi: 10.1103/physreve.77.066205.
- [118] B. Kralemann et al., "In vivo cardiac phase response curve elucidates human respiratory heart rate variability," *Nature Commun.*, vol. 4, no. 1, p. 2418, Sep. 2013, doi: 10.1038/ncomms3418.
- [119] J. H. Zar, "Spearman rank correlation," in *Encyclopedia of Biostatistics*, vol. 7, 2005, doi: 10.1002/0470011815.b2a15150.
- [120] R. Matsuya, J. Ushiyama, and J. Ushiba, "Inhibitory interneuron circuits at cortical and spinal levels are associated with individual differences in corticomuscular coherence during isometric voluntary contraction," *Sci. Rep.*, vol. 7, no. 1, p. 44417, Mar. 2017, doi: 10.1038/srep44417.
- [121] R. G. Abeysuriya et al., "A biophysical model of dynamic balancing of excitation and inhibition in fast oscillatory large-scale networks," *PLOS Comput. Biol.*, vol. 14, no. 2, Feb. 2018, Art. no. e1006007.
- [122] F. A. Torres, M. Otero, C. A. Lea-Carnall, J. Cabral, A. Weinstein, and W. El-Deredy, "Emergence of multiple spontaneous coherent subnetworks from a single configuration of human connectome-coupled oscillators model," bioRxiv, Jan. 2024.
- [123] D. Kudo et al., "Individualized beta-band oscillatory transcranial direct current stimulation over the primary motor cortex enhances corticomuscular coherence and corticospinal excitability in healthy individuals," *Brain Stimulation*, vol. 15, no. 1, pp. 46–52, Jan. 2022, doi: 10.1016/j.brs.2021.11.004.
- [124] J. Prado et al., "Distinct representations of subtraction and multiplication in the neural systems for numerosity and language," *Hum. Brain Mapping*, vol. 32, no. 11, pp. 1932–1947, Nov. 2011, doi: 10.1002/hbm.21159.
- [125] H. Pashler, The Psychology of Attention. Cambridge, MA, USA: MIT Press, 1998.
- [126] I. Koch, E. Poljac, H. Müller, and A. Kiesel, "Cognitive structure, flexibility, and plasticity in human multitasking—An integrative review of dual-task and task-switching research," *Psychol. Bull.*, vol. 144, no. 6, pp. 557–583, Jun. 2018, doi: 10.1037/bul0000144.

- [127] S. T. Christie and P. Schrater, "Cognitive cost as dynamic allocation of energetic resources," *Frontiers Neurosci.*, vol. 9, p. 289, Aug. 2015, doi: 10.3389/fnins.2015.00289.
- [128] B. Hommel, "Dual-task performance: Theoretical analysis and an event-coding account," *J. Cognition*, vol. 3, no. 1, p. 29, Sep. 2020, doi: 10.5334/joc.114.
- [129] J. Volkmann et al., "Central motor loop oscillations in parkinsonian resting tremor revealed magnetoencephalography," *Neurology*, vol. 46, no. 5, p. 1359, May 1996, doi: 10.1212/wnl.46.5.1359.
- [130] P. C. Poortvliet, K. J. Tucker, S. Finnigan, D. Scott, P. Sowman, and P. W. Hodges, "Cortical activity differs between position- and force-control knee extension tasks," *Exp. Brain Res.*, vol. 233, no. 12, pp. 3447–3457, Dec. 2015, doi: 10.1007/s00221-015-4404-8.
- [131] J. T. Gwin and D. P. Ferris, "Beta- and gamma-range human lower limb corticomuscular coherence," *Frontiers Hum. Neurosci.*, vol. 6, p. 258, Sep. 2012, doi: 10.3389/fnhum.2012.00258.
- [132] E. Heinrichs-Graham et al., "Neuromagnetic evidence of abnormal movement-related beta desynchronization in Parkinson's disease," *Cerebral Cortex*, vol. 24, no. 10, pp. 2669–2678, Oct. 2014, doi: 10.1093/cercor/bht121.
- [133] L. Roeder, T. W. Boonstra, and G. K. Kerr, "Corticomuscular control of walking in older people and people with Parkinson's disease," *Sci. Rep.*, vol. 10, no. 1, p. 2980, 2020, doi: 10.1038/s41598-020-59810-w.
- [134] O. Beauchet, V. Dubost, K. Aminian, R. Gonthier, and R. W. Kressig, "Dual-task-related gait changes in the elderly: Does the type of cognitive task matter?" *J. Mot. Behav.*, vol. 37, no. 4, pp. 259–264, Jul. 2005.
- [135] C. Voelcker-Rehage and J. L. Alberts, "Effect of motor practice on dual-task performance in older adults," *J. Gerontol. B, Psychol. Sci. Social Sci.*, vol. 62, no. 3, pp. P141–P148, May 2007, doi: 10.1093/geronb/62.3.p141.
- [136] R. Kristeva-Feige, C. Fritsch, J. Timmer, and C.-H. Lücking, "Effects of attention and precision of exerted force on beta range EEG-EMG synchronization during a maintained motor contraction task," *Clin. Neurophysiol.*, vol. 113, no. 1, pp. 124–131, Jan. 2002, doi: 10.1016/s1388-2457(01)00722-2.
- [137] A. N. Johnson, L. A. Wheaton, and M. Shinohara, "Attenuation of corticomuscular coherence with additional motor or non-motor task," *Clin. Neurophysiol.*, vol. 122, no. 2, pp. 356–363, Feb. 2011, doi: 10.1016/j.clinph.2010.06.021.
- [138] F. Negro and D. Farina, "Linear transmission of cortical oscillations to the neural drive to muscles is mediated by common projections to populations of motoneurons in humans," *J. Physiol.*, vol. 589, no. 3, pp. 629–637, Feb. 2011, doi: 10.1113/jphysiol.2010.202473.
- [139] E. R. Williams and S. N. Baker, "Circuits generating corticomuscular coherence investigated using a biophysically based computational model. I. Descending systems," *J. Neurophysiol.*, vol. 101, no. 1, pp. 31–41, Jan. 2009, doi: 10.1152/jn.90362.2008.
- [140] T. W. Boonstra, B. C. M. van Wijk, P. Praamstra, and A. Daffertshofer, "Corticomuscular and bilateral EMG coherence reflect distinct aspects of neural synchronization," *Neurosci. Lett.*, vol. 463, no. 1, pp. 17–21, Sep. 2009, doi: 10.1016/j.neulet.2009.07.043.
- [141] T. W. Boonstra, "The potential of corticomuscular and intermuscular coherence for research on human motor control," *Frontiers Hum. Neurosci.*, vol. 7, p. 855, Jan. 2013.
- [142] T. D. Aumann and Y. Prut, "Do sensorimotor β-oscillations maintain muscle synergy representations in primary motor cortex?" Trends Neurosci., vol. 38, no. 2, pp. 77–85, Feb. 2015, doi: 10.1016/j.tins.2014.12.002.
- [143] A. Reyes, C. M. Laine, J. J. Kutch, and F. J. Valero-Cuevas, "Beta band corticomuscular drive reflects muscle coordination strategies," *Frontiers Comput. Neurosci.*, vol. 11, p. 17, Apr. 2017, doi: 10.3389/fncom.2017.00017.
- [144] C. S. Zandvoort, J. H. van Dieën, N. Dominici, and A. Daffertshofer, "The human sensorimotor cortex fosters muscle synergies through cortico-synergy coherence," *NeuroImage*, vol. 199, pp. 30–37, Oct. 2019, doi: 10.1016/j.neuroimage.2019.05.041.
- [145] J. Liu et al., "Closed-loop construction and analysis of corticomuscular-cortical functional network after stroke," *IEEE Trans. Med. Imag.*, vol. 41, no. 6, pp. 1575–1586, Jun. 2022, doi: 10.1109/TMI.2022.3143133.
- [146] T. Stankovski, V. Ticcinelli, P. V. E. McClintock, and A. Stefanovska, "Coupling functions in networks of oscillators," *New J. Phys.*, vol. 17, no. 3, Mar. 2015, Art. no. 035002, doi: 10.1088/1367-2630/17/3/035002.
- [147] J. Ushiyama et al., "Between-subject variance in the magnitude of corticomuscular coherence during tonic isometric contraction of the tibialis anterior muscle in healthy young adults," J. Neurophysiol., vol. 106, no. 3, pp. 1379–1388, Sep. 2011, doi: 10.1152/jn.00193.2011.